Synthesis and electroluminescent property of novel europium complexes with oxadiazole substituted 1,10-phenanthroline and 2,2′-bipyridine ligands†

Zhuqi Chen,‡ Fei Ding,‡ Feng Hao, Ming Guan, Zuqiang Bian,* Bei Ding and Chunhui Huang

Received (in Montpellier, France) 7th September 2009, Accepted 10th November 2009
First published as an Advance Article on the web 13th January 2010
DOI: 10.1039/b9nj00461k

Several 1,10-phenanthroline derivatives (PhoR), 2,2′-bipyridine derivatives (BpoR) and related europium complexes $Eu(TTA)_3PhoR$ and $Eu(TTA)_3BpoR$ were synthesized (HTTA = 2-thenoyltrifluoroacetone). Single crystal X-ray diffraction of $Eu(TTA)_3Php$ (Php = 2-(pyridyl)-1,10-phenanthroline) shows that Php acts as a tridentate $N\hat{}N\hat{}N$ ligand, leading to a high stability of the complex for vacuum evaporation. When an oxadiazole moiety is incorporated into the ligand, the corresponding europium complexes show improved carrier-transporting abilities as well as thermal stabilities under vapor deposition for electroluminescence (EL) applications. Experiments revealed that these complexes have high photoluminescence (PL) quantum yields due to suitable triplet energy levels (E_T) of the ligands, between 19 724 and 22 472 cm^{-1}, for the sensitization of Eu(III) ($^5D_0$: 17 500 cm^{-1}). Utilizing $Eu(TTA)_3PhoB$ (PhoB = 2-(5-phenyl-1,3,4-oxadiazol-2-yl)-1,10-phenanthroline) as the dopant emitter in CBP (4,4′-*N*,*N*′-dicarbazolebiphenyl), EL devices with a structure of TPD (4,4′-bis[*N*-(*p*-tolyl)-*N*-phenylamino] biphenyl, 30 nm)/$Eu(TTA)_3PhoB$:CBP (7.5%, 20nm)/BCP (2,9-dimethyl-4,7-diphenyl-1,10-phenanthroline, 20 nm)/Alq_3 (tris(8-hydroxyquinoline), 30 nm) exhibited a pure emission from europium ions. The highest efficiency obtained was 5.5 lm W^{-1}, 8.7 cd A^{-1} and the maximum brightness achieved was 1086 cd m^{-2}. At a practical brightness of 100 cd m^{-2}, the efficiency remains above 2.0 cd A^{-1}.

Introduction

For organic electroluminescence (EL) devices, the development of high-performance red emission is still much in demand. Rare earth complexes have been used as emitters in organic light-emitting diodes (OLEDs) due to their sharp-band emissions and high photoluminescence (PL) quantum yields.[1–5] Many europium complexes have been investigated because they are known as excellent red phosphors that exhibit intense sharp red light at around 613 nm while other red organic emitting materials give broad emission spectra with bandwidths of around 100 nm resulting dull colors.[6–14] However, OLEDs based on europium(III) complexes do not show satisfying brightness and efficiency due to their poor carrier transporting abilities.[2,11] There are two methods of modification: one is introducing carrier transporting groups to ligands,[15–20] the other is doping europium complexes into host materials with good semiconductor properties.[11,21–25] Indeed, the EL efficiencies of europium complex-based OLEDs were enhanced through the above methods. However, the performances achieved are not satisfactory compared to organic molecules and polymer-based LEDs. Therefore, further improvement of OLEDs based on europium complexes is of great importance. When carrier transporting groups are introduced to the ligands, high molecular weights bring another key problem: volatilities and thermal stabilities of europium complexes during the vacuum evaporation.[26,27] After all, while many advances have been made, europium complexes including high quantum efficiencies, good carrier transporting abilities and thermal abilities for deposition are still in demand. Based on these considerations, novel 1,10-phenanthroline and 2,2′-bipyridine derivatives and related europium complexes were designed and synthesized. By single crystal X-ray diffraction we confirm that 2-(pyridyl)-1,10-phenanthroline (Php) offers three coordination atoms which contribute to a high stability of the related complex.[28,29] The pyridine moiety is further replaced by an oxadiazole moiety, which have been proven to be very effective in improving the injection and transport of electrons.[30–32] By comparing element analysis data of the complex before and after sublimation, we figure that europium complexes with these oxadiazole substituted ligands maintain thermal stability for deposition. Furthermore, the triplet energy levels (E_T) of the ligands are suitable for complete energy transfer to central ions, which leads to high quantum yields of related complexes. The utilization of these novel

Beijing National Laboratory for Molecular Sciences, State Key Laboratory of Rare Earth Materials Chemistry and Applications, College of Chemistry and Molecular Engineering, Peking University, 100871, Beijing, China. E-mail: bianzq@pku.edu.cn; Fax: +86 10-6275-7156; Tel: +86 10-6275-7156

† Electronic supplementary information (ESI) available: Excitation spectra of complexes $Eu(TTA)_3BpoR$ and $Eu(TTA)_3PhoR$ in CH_2Cl_2. CCDC reference numbers 754692. For ESI and crystallographic data in CIF or other electronic format see DOI: 10.1039/b9nj00461k

‡ These authors contributed equally to this work.

complexes as red emitters in EL devices are explored and remarkable performances are achieved.

Results and discussion

As shown in Scheme 1, Compounds **1**, **2** and **3** were synthesized according to reported procedures.[33,34] Reaction of compound **3** with a variety of benzoyl chloride derivatives afforded the neutral ligands. Then, based on the well-known formation of eight-coordinate adducts between {Ln(dik)$_3$} units and *N*,*N*-bidentate chelates, europium complexes Eu(TTA)$_3$Php, Eu(TTA)$_3$PhoR and Eu(TTA)$_3$BpoR were synthesized and characterized. Details were described in the experimental section.

Crystal and molecular structure

Single crystals of Eu(TTA)$_3$Php were isolated from acetone and ethanol solutions and analyzed by X-ray diffraction. The X-ray diffraction data were collected on a Rigaku MicroMax-007 CCD diffractometer by the ω scan technique at 131 K using graphite-monochromated Mo/Kα (λ = 0.71073 Å) radiation. An absorption correction by multiscan was applied to the intensity data. The structures were solved by the direct method, and the heavy atoms were located from the E-map. The remaining nonhydrogen atoms were determined from the successive difference Fourier syntheses. The non-hydrogen atoms were refined anisotropically, whereas the hydrogen atoms were generated geometrically with isotropic thermal parameters. The structures were refined on F^2 by full-matrix least-squares methods using the SHELXTL-97 program package.

The europium ion was surrounded by six oxygen atoms from the bidentate β-diketonate ligands and three nitrogen atoms from the neutral ligand Php (Fig .1). The coordination polyhedron can be described as a distorted square antiprism. The lengths of Eu–N are 2.596(4), 2.650(4) and 2.603(4) Å. They are shorter than those in previous reports of *N*^*N*^*N* ligand based europium complexes (2.68, 2.70 and 2.72 Å) in the literature.[35–37] Shorter bond lengths suggest higher stability, which is presumed by the rigid structure of the phenanthroline moiety.

Thermal stability for deposition

The chemical weight of materials increasing upon the introduction of modification groups usually leads to difficulty in evaporation of the complexes in vacuum. Previous reports showed that the neutral ligand phenanthroline was slightly dissociated in vapor deposition and the residue in the crucible became dark.[26,27] We compare the element analysis data of both the products of europium complexes from sublimation and residues left in the crucible. For Eu(TTA)$_3$Phen, an obvious decrease of C, H, and N contents of the product after sublimation is observed (Table 1). The products were presumed to be a mixture of Eu(TTA)$_3$Phen and Eu(TTA)$_3$. The neutral ligand dissociates in the sublimation process. Meanwhile, Eu(TTA)$_3$PhoR remains as a white powder after vacuum evaporation for many times. Taking Eu(TTA)$_3$PhoB as an example, we compared the elemental analysis data of both the product from vacuum evaporation and the residue. They were both coincident with calculated values. The melting points (T_m) and the thermal decomposition temperatures (T_d) of the complexes are also measured and are listed in Table 2. No glass transition temperature or crystallization temperature is found in any of these complexes. Thus, with the substituted 1,3,4-oxadiazole group, Eu(TTA)$_3$PhoR shows the desired thermal stability for deposition. This stability makes devices fabricated by vacuum evaporation more feasible.

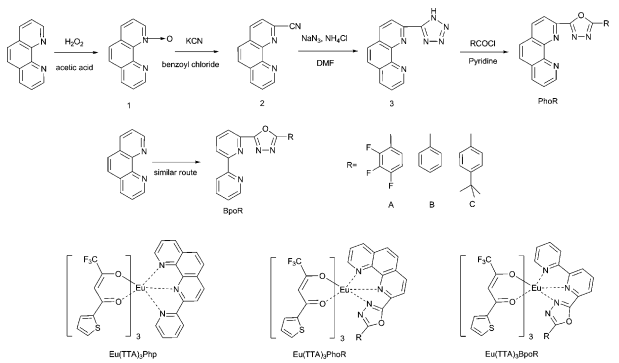

Scheme 1 Synthetic routes, chemical structures and corresponding abbreviations of the neutral ligands and europium complexes.

Table 1 Element analysis data of europium complexes

Complexes	Products from sublimation	Residue left in crucible	Calculated values[a]
Eu(TTA)$_3$PhoB ($C_{44}H_{24}EuF_9N_4O_7S_3$)	C: 46.43 H: 2.27 N: 4.80	C: 46.05 H: 2.10 N: 4.92	C: 46.36 H: 2.12 N: 4.92
Eu(TTA)$_3$Phen ($C_{36}H_{20}EuF_9N_2O_6S_3$)	C: 40.23 H: 1.83 N: 2.43	C: 50.12 H: 3.26 N: 1.39	C: 44.49 H: 2.55 N: 2.73
Eu(TTA)$_3$ ($C_{24}H_{12}EuF_9O_6S_3$)			C: 35.35 H: 1.48 N: —

[a] According to the molecular formula.

Photophysical studies

For further research on EL properties of corresponding europium complexes, their photophysical properties were investigated. We focused more on the oxadiazole substituted

Table 2 Thermal stabilities and photophysical data of Eu complexes

Complexes	T_d/°C	T_m/°C	λ_{max}(abs)/nm (ε/dm^3 mol^{-1} cm^{-1})
Eu(TTA)$_3$Php	290.5	242	303 (35 971) 341 (33 854)
Eu(TTA)$_3$PhoA	282.8	239	304 (43 040) 343 (45 710)
Eu(TTA)$_3$PhoB	327.2	261	269 (31 820) 308 (45 520) 343 (55 030)
Eu(TTA)$_3$PhoC	307.9	262	266 (30 260) 345 (46 480)
Eu(TTA)$_3$BpoA	281.4	224	271 (42 210) 345 (40 610)
Eu(TTA)$_3$BpoB	285.6	227	274 (53 760) 343 (46 980)
Eu(TTA)$_3$BpoC	293.9	231	275 (40 910) 345 (52 980)

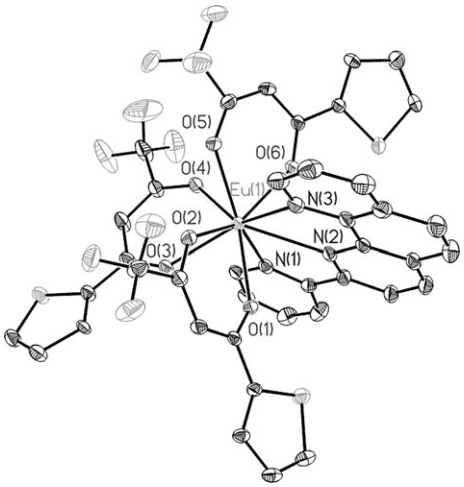

Fig. 1 An ORTEP view of the crystal structure of $Eu(TTA)_3Php$ with partial atomic labeling. Thermal ellipsoids are drawn at the 30% probability level.

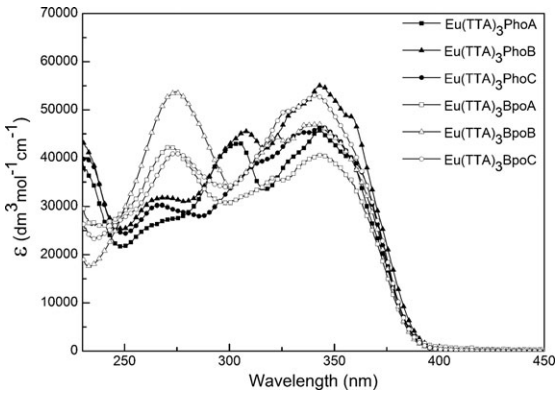

Fig. 2 Absorption spectra of europium complexes in CH_2Cl_2 (10^{-5} mol L^{-1}).

ligands (PhoR and BpoR) rather than on Php, which had been reported before.[34,38] The absorption spectra of europium complexes in CH_2Cl_2 (10^{-5} mol L^{-1}) at room temperature are shown in Fig. 2. Similar absorption bands of $Eu(TTA)_3PhoR$ were observed at about 264 nm and 305 nm, while those of $Eu(TTA)_3BpoR$ were observed at 275 nm and 322 nm. These broad absorption bands are due to both TTA and neutral ligands.[14] All of the complexes show the same lowest absorption maximums at about 340 nm and their low energy absorption edges at 390–400 nm. This distinct absorption band is probably assigned to the $\pi \rightarrow \pi^*$ transition of the anionic ligand TTA.[39]

The PL spectra of the complexes show characteristic europium ion emissions at λ = 579 nm ($^5D_0 \rightarrow {}^7F_0$), 588–597 nm ($^5D_0 \rightarrow {}^7F_1$), 613–620 nm ($^5D_0 \rightarrow {}^7F_2$), 650 nm ($^5D_0 \rightarrow {}^7F_3$) and 692 nm ($^5D_0 \rightarrow {}^7F_4$) (Fig. 3). Since the $^7F_0$ state of Eu^{3+} is nondegenerate, the $^5D_0 \rightarrow {}^7F_0$ transition can not be split by the ligand field. Therefore, the single peak at 579 nm in the emission spectrum indicates that there is only one luminescent Eu^{3+} species in solution.[40] The splitting of the $^5D_0 \rightarrow {}^7F_1$ and $^5D_0 \rightarrow {}^7F_2$ transition, caused by the ligand field, is about 200 cm^{-1} and the intensity ratio of $^5D_0 \rightarrow {}^7F_2$ transition and $^5D_0 \rightarrow {}^7F_1$ transition (I_{7F2}/I_{7F1}) is about 19.

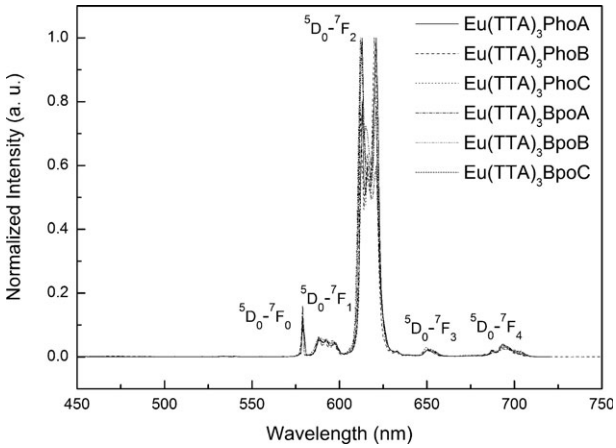

Fig. 3 PL spectra of europium complexes in CH_2Cl_2 (10^{-5} mol L^{-1}).

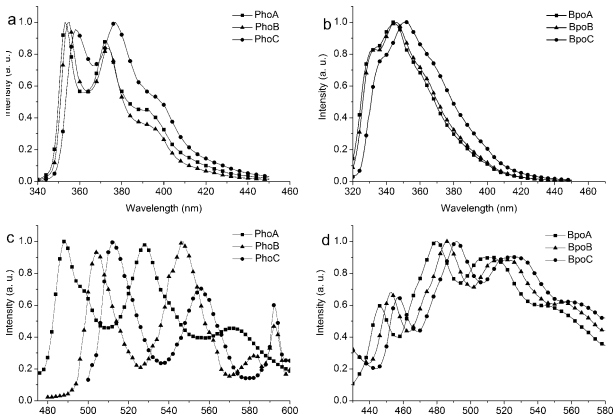

Fig. 4 Fluorescence spectra of the ligands (a, b) in CH_2Cl_2 (10^{-5} mol L^{-1}) and phosphorescence spectra of the related gadolinium complexes in ethanol (10^{-5} mol L^{-1}) at 78 K (c, d).

Since the distortion of the symmetry around the central ion causes an intensity enhancement of the hypersensitive $^5D_0 \rightarrow {}^7F_2$ transition and the intensity of the $^5D_0 \rightarrow {}^7F_1$ transition is independent of the coordination sphere, the high I_{7F2}/I_{7F1} indicates that the symmetry of the coordination sphere is low.[41]

It is known that the sensitization pathway in lanthanide complexes generally consists of excitation of the ligand into its singlet excited state, subsequent intersystem crossing to its triplet state and energy transfer from the triplet state of the ligand to the lanthanide ion.[40,42,43] The singlet energy levels (E_S) and triplet energy levels (E_T) of the ligands and the PL

Table 3 Singlet and triplet state energy levels of the ligands and quantum yields (Φ) of related europium complexes

Ligand	E_S/cm^{-1}	E_T/cm^{-1}	$E_T-{}^5D_0/cm^{-1}$	Φ^a
PhoA	28 329	20 492	2992	30%
PhoB	28 169	19 841	2341	40%
PhoC	26 525	19 724	2224	42%
BpoA	29 070	22 472	4972	16%
BpoB	28 902	22 075	4574	22%
BpoC	28 409	21 882	4382	26%

[a] Measured in CH_2Cl_2 by using $Ru(bpy)_3Cl_2$ distilled water as a reference compound (ref. 44).

quantum yields (Φ) of the related complexes were measured (Fig. 4) and are listed in Table 3. The singlet energy levels were determined by fluorescence spectra of the ligands (10^{-5} mol L^{-1} in CH_2Cl_2, room temperature). The phosphorescence spectra of the related gadolinium complexes (10^{-5} mol L^{-1} in ethanol, 78 K) reveal the lowest triplet energy levels of the ligands because the lowest excited state $^6P_{7/2}$ energy of Gd(III) is too high to accept energy from the ligands. PhoA with three fluoro substituents as an electron drawing group shows higher E_T (20 492 cm^{-1}) than that of PhoB (19 841 cm^{-1}) while PhoC with *tert*-butyl as an electron pushing group shows lower E_T (19 724 cm^{-1}). All of three ligands show a lower E_T than phenanthroline (21 480 cm^{-1}),[41] as the π-system of the ligand is extended by the oxadiazole group. Moreover, the fluorescence peaks of PhoA and PhoC show hypsochromic and bathochromic shifts compared with that of PhoB, respectively. This confirms that the addition of the electron-pushing *tert*-butyl group or the electron-withdrawing fluorine substituents on the phenyl ring alters the electronic density of the π-system; therefore, they reduce or increase both the singlet and the triplet energy level of the ligand. A similar phenomenon is observed in bipyridine derivatives and all of them show a lower E_T than that of bipyridine (22 900 cm^{-1}).[44] As all of these complexes have similar coordination environments, the suitability of the energy gap between the triplet energy level of the ligand and the main luminescent energy level of the central ion ($^5D_0$ for Eu^{3+}: 17 500 cm^{-1}) is therefore critical for the efficiency of the energy transfer. By comparing the energy gaps and the quantum yields (Table 3), a general tendency is observed that a smaller energy gap (E_T–$^5D_0$) leads to a higher quantum yield of the related complex.

Electroluminescent properties

By introducing TPD and Alq_3 as hole and electron transporting materials, respectively, and BCP as a hole blocking material, EL device A1 was fabricated. $Eu(TTA)_3(PhoB)$ was chose as the emitter for its high PL quantum yield as well as its good thermal stability. The structures and the performances of devices are listed in Table 4. Compared with previous reports of non-doped OLEDs based on $Eu(TTA)_3Phen$,[11,46] a higher brightness of 32 cd m^{-2} (160 mA cm^{-2}) is achieved at a lower applied voltage (14 V). The EL spectra at high voltages show broad peaks at 660 nm (Fig. 5). Device A2 was fabricated with a CBP film complementing as a hole-transporting layer (HTL). Compared to device A1, the intensity of the broad peak at high wavelength

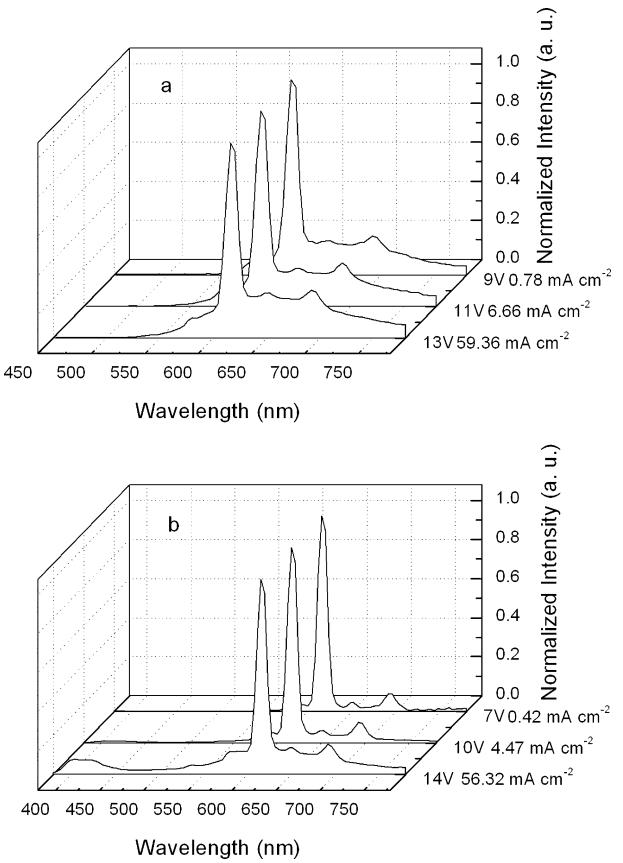

Fig. 5 EL spectra of device A1 (a) and A2 (b) at different voltages.

Table 4 Performances of Eu complexes based OLEDs[a]

Device	Device structure	Turn-on voltage/V	L [cd m^2, V]	η_c [cd A^{-1}, V]	η_p [lm W^{-1}, V]	CIE, 10 cd m^{-2}(x, y)
A1	TPD (30 nm)/$Eu(TTA)_3$PhoB (30 nm)/ BCP (5 nm)/Alq_3 (30 nm)	9	32, 14	0.05,10	0.017,10	0.65, 0.35
A2	TPD (30 nm)/CBP (5 nm)/$Eu(TTA)_3$PhoB (30 nm)/BCP (5 nm)/Alq_3 (30 nm)	6	67, 14	0.53, 7	0.24,7	0.65, 0.33
B1	NPB (25 nm)/$Eu(TTA)_3$PhoB:CBP (3%, 25 nm)/BCP (15 nm)/Alq_3 (35 nm)	9	703, 18	3.0, 10	0.90,10	0.65, 0.32
B2	NPB (25 nm)/$Eu(TTA)_3$PhoC:CBP (3%, 25 nm)/BCP (15 nm)/Alq_3 (40 nm)	9	421, 20	2.56, 9	0.89, 9	0.63. 0.31
B3	NPB (25 nm)/$Eu(TTA)_3$BpoB:CBP (3%, 25 nm)/BCP (15 nm)/Alq_3 (30 nm)	10	424, 53	1.37,17	0.26,17	0.63. 0.31
C1	TPD (30 nm)/$Eu(TTA)_3$PhoB:CBP (2.2%, 20 nm)/BCP(20 nm)/Alq_3 (30 nm)	6	1099, 20	2.6, 10	0.8, 10	0.65, 0.32
C2	TPD (30 nm)/$Eu(TTA)_3$PhoB:CBP (4.2%, 20 nm)/BCP (20 nm)/Alq_3 (30 nm)	5	877, 19	8.7, 6	3.9, 6	0.64, 0.32
C3	TPD (30 nm)/$Eu(TTA)_3$PhoB:CBP (7.5%, 20 nm)/BCP (20 nm)/Alq_3 (30 nm)	4	1086, 17	8.7, 5	5.5, 5	0.65, 0.32

[a] The data for brightness (L), current efficiency (η_c), and power efficiency (η_p) are the maximum values of devices.

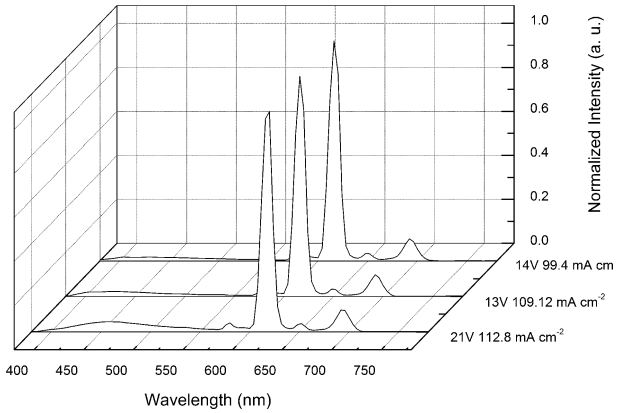

Fig. 6 EL spectra of device B1, C1 and C2 at similar current densities.

decreases but an emission centered at 420 nm arises at high voltages in device A2. Thus, we presume that the broad peak at 660 nm is attributable to an exciplex of $Eu(TTA)_3PhoB$ and TPD. Moreover, it also demonstrates that the substituted 1,3,4-oxadiazole group is favorable to increase the electron-transporting ability of the complex, thus the carriers are mainly recombined between EML and HTL in these devices.

To avoid the exciplex at high voltages, NPB was used instead of TPD as a hole transporting material. Three devices B1–B3 with $Eu(TTA)_3PhoB$, $Eu(TTA)_3PhoC$, and $Eu(TTA)_3BpoB$ as dopant emitters in CBP (3%) were fabricated, respectively. All of the EL spectra of these devices show a strong emission of europium ions at 612 nm while an emission centered at 420 nm is observed at high voltages, similar to the spectrum of device A2. This additional purple-blue emission can be attributed to the direct emission from CBP.[11] In device B1 a maximum brightness of 703 cd m^{-2} at 18 V, a current efficiency of 3.0 cd A^{-1} and a power efficiency of 0.90 lm W^{-1} at 10 V are achieved. In device B2 and B3, $Eu(TTA)_3PhoC$ and $Eu(TTA)_3BpoB$ are used instead of $Eu(TTA)_3PhoB$, respectively. Device B2 shows a similar performance with a maximum brightness of 421 cd m^{-2} at 20 V, a current efficiency of 2.56 cd A^{-1} and a power efficiency of 0.89 lm W^{-1} at 9 V. However, the current efficiency and the power efficiency of device B3 is 1.37 cd A^{-1} and 0.26 lm W^{-1}. This performance is consistent with their different PL quantum yields (Table 3). Strong roll-off characteristics of efficiencies at high voltages are observed in all devices (Fig. 7). The phenomenon is thought to be a result of some processes quenching the excited states.[10,11,47]

Using $Eu(TTA)_3PhoB$ as the guest emitter with concentrations from 2.2% to 7.5% in CBP, devices C1–C3 are fabricated. The structure was ITO/TPD (30 nm)/$Eu(TTA)_3PhoB$:CBP (X%, 20 nm)/BCP (20 nm)/AlQ (30 nm)/$Mg_{0.9}Ag_{0.1}$. EL spectra of device C1 and C2 show a characteristic red emission of $Eu(TTA)_3PhoB$ with a weak emission at 420 nm (Fig. 6). All of the devices have maximum brightness around 1000 cd m^{-2}. As the concentration of $Eu(TTA)_3PhoB$ is increased from 2.2% (device C1) to 7.5% (device C3), more excitons are contributed to the lanthanide luminescence process. A higher PL quantum yield of the lanthanide complexes (100% theoretical quantum efficiency) leads to

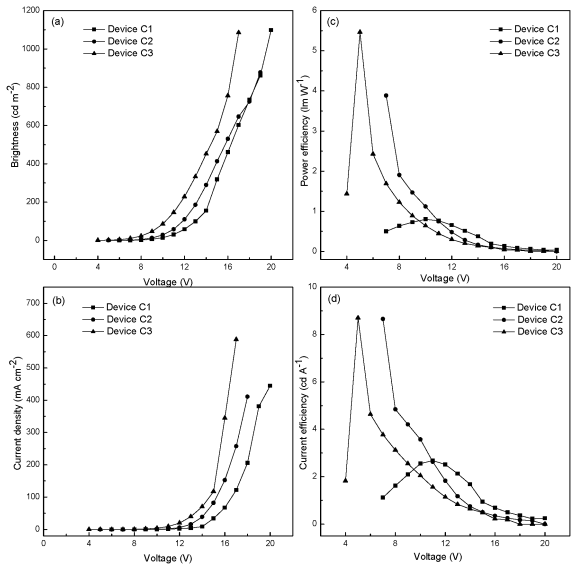

Fig. 7 EL performance of device C1–C3: brightness (a), current density (b), power efficiency (c) and current efficiency (d) *versus* voltage.

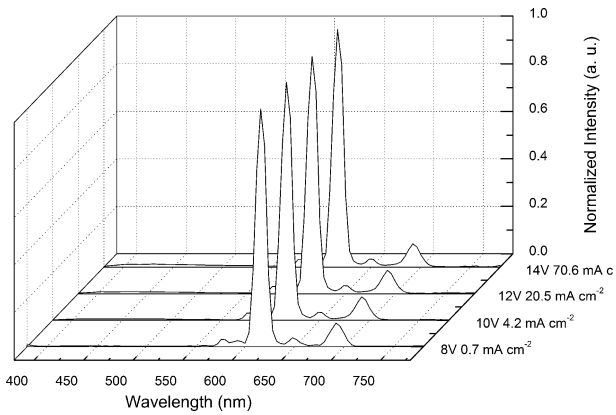

Fig. 8 EL spectra of device C3 at different applied voltages.

higher EL efficiencies. Hence, the power efficiency and the current efficiency increase from 0.8 lm W^{-1} and 2.6 cd A^{-1} (device C1) to 5.5 lm W^{-1} and 8.7 cd A^{-1} (device C3) (Table 4). Device C3 shows a purer emission that originates from the europium complex. Even at the highest applied voltage, only a trace emission at 450 nm is observed (Fig. 8). This reveals that carriers are well confined within the emitting layer and the energy transfer between CBP and $Eu(TTA)_3PhoB$ is complete in this device. Thus, a remarkable performance of device C3 is achieved.

Experimental

Methods and instruments

Alq_3 was synthesized according to literature procedures[48] and sublimed twice prior to use. CBP, NPB, TPD and BCP were purchased from Aldrich and used after sublimation. $Eu(TTA)_3Phen$ and $Eu(TTA)_3(H_2O)_2$ were synthesized according to a previous report.[49] Chromatographic separation

was carried out on silica gel (200–300 mesh) for purification. The ^{1}H NMR spectra were recorded on a Varian 400 MHz instrument using Me_4Si as an internal reference. Mass spectra were recorded on a ZAB-HS and BIFLEX III. Elemental analyses were performed on a VARIO EL analyzer. Thermogravimetric and differential thermal analysis were carried out on Q600SDT and Q100DSC instruments at an elevation temperature rate of 10 °C min^{-1} under 100 mL min^{-1} nitrogen flow. EL and PL spectra were recorded with an Edinburgh Analytical Instruments FLS920 spectrometer after removing oxygen in the solution by a vacuum technique (3 or 4 freeze–pump–thaw cycles). Absorption spectra were measured on a Shimadzu UV-3100 UV-vis spectrometer. Solvents for reactions were distilled prior to use. Solvents used in photophysical experiments were of spectroscopic grade.

General procedure for the synthesis of the neutral ligands

2-(pyridyl)-1,10-phenanthroline, 1,10-phenanthroline 1-oxide (**1**) and 2-cyano-1,10-phenanthroline (**2**) were synthesized according to reported procedures.[33,34] Compound **2** (4.1 g, 20 mmol), sodium azide (2.93 g, 45 mmol) and ammonium chloride (2.4 g, 45 mmol) in 30 ml of DMF was heated at 100 °C for 24 h. After cooling to room temperature the mixture was poured into 400 ml of water and acidified with dilute HCl. The resulting white precipitate was collected, washed with water, and dried in vacuum at 60 °C, yielding 2-(1*H*-tetrazol-5-yl)-1,10-phenanthroline (**3**).[50] The benzoyl chloride derivative (22 mmol) was then added to a solution of **3** (4.96 g, 20 mmol) in 25 ml of pyridine, and the mixture was refluxed for 2 h under nitrogen flow. 200 mL of water was added to the cooled reaction mixture affording a white precipitate. The precipitate was isolated, washed with water and dried in vacuum at 60 °C. The 5-(1*H*-tetrazol-5-yl)-2,2′-bipyridine was synthesized with the same procedure of **3**. Bipyridine derivatives were then synthesized with the same benzoyl chloride derivatives. The individual yields and important spectral data of these products are listed below.

2-(1*H*-tetrazol-5-yl)-1,10-phenanthroline (3). Yield: 72%. ^{1}H NMR (400 MHz, DMSO-d_6), 9.44–9.42 (q, 1H), 9.28–9.26 (d, 1H), 8.92–8.90 (d, 1H), 8.65–8.63 (d, 1H), 8.38–8.33 (m, 3H), MS (*m*/*z*): calcd. for $C_{13}H_8N_6$ 248, found 248.

5-(1*H*-tetrazol-5-yl)-2,2′-bipyridine. Yield: 78%. ^{1}H NMR (400 MHz, DMSO-d_6), 8.84–8.82 (d, 1H), 8.75–8.74 (d, 1H), 8.60–8.57 (d, 1H), 8.28–8.20 (m, 2H), 8.09–8.05 (t, 1H),7.55–7.54 (t, 1H), MS (*m*/*z*): calcd. for $C_{11}H_8N_6$ 224, found 224.

2-(5-(2,3,4-trifluorophenyl)-1,3,4-oxadiazol-2-yl)-1,10-phenanthroline (PhoA). Yield: 60%. ^{1}H NMR (400 MHz, $CDCl_3$), 9.31–9.29 (q, 1H), 8.70–8.6 7(d, 1H), 8.51–8.49 (d, 1H), 8.37–8.34 (q, 1H), 8.19–8.13 (m, 1H), 7.97–7.91 (q, 2H), 7.77–7.74 (q, 1H), 7.26–7.18 (m, 1H), MS (*m*/*z*): calcd. for $C_{20}H_9F_3N_4O$ 378, found 378. Anal. calcd. for $C_{20}H_9F_3N_4O$: C, 63.50; H, 2.40; N, 14.81. Found: C, 63.50; H, 2.49; N, 14.88.

2-(5-phenyl-1,3,4-oxadiazol-2-yl)-1,10-phenanthroline (PhoB). Yield: 80%. ^{1}H NMR (400 MHz, $CDCl_3$), 9.23–9.22 (q, 1H), 8.79–8.77 (d, 1H), 8.62–8.60 (d, 1H), 8.58–8.56 (q, 1H), 8.23–8.20 (q, 2H), 8.16–8.11 (q, 2H), 7.88–7.85 (d, 1H), 7.72–7.69 (m, 3H), MS (*m*/*z*): calcd. for $C_{20}H_{12}N_4O$ 324, found 324. Anal. calcd. for $C_{20}H_{12}N_4O$: C, 74.06; H, 3.73; N, 17.27. Found: C, 74.09; H, 3.76; N, 17.04. ^{13}C NMR (400 MHz, $CDCl_3$), 165.99 (C), 164.22 (C), 150.62 (CH), 145.86 (C), 145.55 (C), 143.25 (C), 137.33 (C), 136.29 (C), 131.92 (CH), 129.48 (C), 129.03 (CH), 128.82 (CH), 128.37 (CH), 127.56 (CH), 126.06 (CH), 123.50 (CH), 123.44 (CH), 122.13 (CH).

2-(5-(4-*tert*-butylphenyl)-1,3,4-oxadiazol-2-yl)-1,10-phenanthroline (PhoC). Yield: 60%. ^{1}H NMR (400 MHz, $CDCl_3$), 9.30–9.29 (q, 1H), 8.70–8.67 (d, 1H), 8.47–8.45 (d, 1H), 8.34–8.29 (m, 3H), 7.94–7.88 (q, 2H), 7.94–7.88 (q, 2H), 7.74–7.71 (q, 1H), 7.58–7.56 (m, 2H), 1.39 (s, 9H), MS (*m*/*z*): calcd. for $C_{24}H_{20}N_4O$ 380, found 380. Anal. calcd. for $C_{24}H_{20}N_4O$: C, 75.77; H, 5.30; N, 14.73. Found: C, 75.66; H, 5.26; N, 14.72. ^{13}C NMR (400 MHz, $CDCl_3$), 166.02 (C), 163.98 (C), 155.44 (C), 150.59 (CH), 145.83 (C), 145.58 (C), 143.30 (C), 137.20 (C), 136.07 (C), 129.32 (C), 128.91 (CH), 128.23 (CH), 127.72 (CH), 125.92 (CH), 125.70 (CH), 123.36 (CH), 122.03 (CH), 120.54 (CH), 34.91 (C), 30.92 (CH_3).

5-(5-(2,3,4-trifluorophenyl)-1,3,4-oxadiazol-2-yl)-2,2′-bipyridine (BpoA). Yield: 57%. ^{1}H NMR (400 MHz, $CDCl_3$), 8.73–8.71 (d, 1H), 8.66–8.61 (q, 2H), 8.32–8.30 (d, 1H), 8.06–8.00 (m, 2H), 8.00–7.8 8(t, 1H), 7.40–7.37 (t, 1H), 7.22–7.18 (m, 1H). MS (*m*/*z*): calcd. for $C_{18}H_9F_3N_4O$ 354, found 354. Anal. calcd. for $C_{18}H_9F_3N_4O$: C, 61.02; H, 2.56; N, 15.81. Found: C, 61.09; H, 2.58; N, 15.77.

5-(5-phenyl-1,3,4-oxadiazol-2-yl)-2,2′-bipyridine (BpoB). Yield: 75%. ^{1}H NMR (400 MHz, $CDCl_3$), 8.74–8.73 (d, 1H), 8.67–8.63 (t, 2H), 8.33–8.31 (d, 1H), 8.26–8.24 (m, 2H), 8.06–7.02 (t, 1H), 7.95–7.91 (t, 1H), 7.62–7.55 (m, 3H), 7.42–7.39 (t, 1H). MS (*m*/*z*): calcd. for $C_{18}H_{12}N_4O$ 300, found 300. Anal. calcd. for $C_{18}H_{12}N_4O$: C, 71.99; H, 4.03; N, 18.66. Found: C, 71.86; H, 4.08; N, 18.28. ^{13}C NMR (400 MHz, $CDCl_3$), 165.30 (C), 163.85 (C), 156.52 (C), 154.84 (C), 149.10 (CH), 142.85 (C), 137.92 (C), 136.92 (CH), 131.83 (CH), 128.94 (CH), 127.11 (CH), 124.21 (CH), 123.64 (CH), 122.90 (CH), 122.88 (CH), 121.41 (CH).

5-(5-(4-*tert*-butylphenyl)-1,3,4-oxadiazol-2-yl)-2,2′-bipyridine (BpoC). Yield: 81%. ^{1}H NMR (400 MHz, $CDCl_3$), 8.73–8.71 (d, 1H), 8.66–8.60 (q, 2H), 8.31–8.29 (d, 1H), 8.18–8.15 (d, 2H), 8.04–8.01 (t, 1H), 7.93–7.88 (t, 1H), 7.59–7.57 (d, 2H), 7.40–7.37 (t, 1H), 1.39 (s, 9H), MS (*m*/*z*): calcd. for $C_{22}H_{20}N_4O$ 356, found 356. Anal. calcd. for $C_{22}H_{20}N_4O$: C, 74.14; H, 5.66; N, 15.72. Found: C, 74.09; H, 5.63; N, 15.67. Anal. calcd. for $C_{18}H_{12}N_4O$: C, 71.99; H, 4.03; N, 18.66. Found: C, 71.86; H, 4.08; N, 18.28. ^{13}C NMR (400 MHz, $CDCl_3$), 165.37 (C), 163.64 (C), 156.45 (C), 155.41 (C), 154.86 (C), 149.06 (CH), 142.93 (C), 137.86 (C), 136.87 (CH), 126.94 (CH), 125.90 (CH), 124.15 (CH), 122.82 (CH), 122.74 (CH), 121.37 (CH), 120.81 (CH), 34.69 (C), 30.97 (CH_3).

General procedure for the synthesis of europium complexes[51]

To a 100 ml side-arm flask under nitrogen, 2-thenoyltrifluoroancetone (0.916 g, 3 mmol), 2,2′-bipyridine or 1,10-phenanthroline

(1 mmol) derivative (BpoR or PhoR), sodium hydroxide (0.12 g, 3 mmol) and 30 ml ethanol were added. The mixture was stirred at 60 °C, while 10 ml ethanol solution of $EuCl_3 \cdot 6H_2O$ (0.366 g, 1.00 mol) was added dropwise. The reaction mixture was heated and stirred at 60 °C for 2 h, and was then cooled to room temperature. The resulting precipitate was filtered off, then washed with water and cool ethanol in turn. The crude product was purified by recrystallization from ethanol solution. The yields and element analysis data of these products are presented below.

Eu(TTA)$_3$(Php). Yield: 83%, Anal. calcd. for $C_{41}H_{23}EuF_9N_3O_6S_3$: C, 45.90; H, 2.16; N, 3.92. Found: C, 45.79; H, 2.13; N, 3.93.

Eu(TTA)$_3$(PhoA). Yield: 83%, Anal. calcd. for $C_{44}H_{21}EuF_9N_4O_7S_3$: C, 44.27; H, 1.77; N, 4.69. Found: C, 44.19; H, 1.78; N, 4.78.

Eu(TTA)$_3$(PhoB). Yield: 76%, Anal. calcd. for $C_{44}H_{24}EuF_9N_4O_7S_3$: C, 46.36; H, 2.12; N, 4.92. Found: C, 46.44; H, 2.09; N, 4.97.

Eu(TTA)$_3$(PhoC). Yield: 83%, Anal. calcd. for $C_{48}H_{32}EuF_9N_4O_7S_3$: C, 48.21; H, 2.70; N, 4.68. Found: C, 48.15; H, 2.74; N, 4.75.

Eu(TTA)$_3$(BpoA). Yield: 85%, Anal. calcd. for $C_{42}H_{21}EuF_9N_4O_7S_3$: C, 43.12; H, 1.81; N, 4.79. Found: C, 43.05; H, 1.85; N, 4.84.

Eu(TTA)$_3$(BpoB). Yield: 79%, Anal. calcd. for $C_{42}H_{24}EuF_9N_4O_7S_3$: C, 45.21; H, 2.17; N, 5.02. Found: C, 45.13; H, 2.18; N, 4.97.

Eu(TTA)$_3$(BpoC). Yield: 80%, Anal. calcd. for $C_{46}H_{32}EuF_9N_4O_7S_3$: C, 47.14; H, 2.75; N, 4.78. Found: C, 47.02; H, 2.80; N, 4.88.

General procedure for the synthesis of gadolinium complexes

2,2′-Bipyridine or 1,10-phenanthroline (1 mmol) derivative (PhoR or BpoR) and $GdCl_3 \cdot 6H_2O$ (0.370 g, 1.00 mol) were heated and stirred at 60 °C for 2 h, and then cooled to room temperature. The product was purified by recrystallization from an ethanol–water mixed solution. The element analysis data of these products are presented below.

GdCl$_3$(PhoA). Anal. calcd. for $C_{20}H_9Cl_3F_3GdN_4O$: C, 37.42; H, 1.41; N, 8.73. Found: C, 37.69; H, 1.48; N, 8.61.

GdCl$_3$(PhoB). Anal. calcd. for $C_{20}H_{12}Cl_3GdN_4O$: C, 40.86; H, 2.06; N, 9.53. Found: C, 40.97; H, 2.15; N, 9.40.

GdCl$_3$(PhoC). Anal. calcd. for $C_{24}H_{20}Cl_3GdN_4O$: C, 44.76; H, 3.13; N, 8.70. Found: C, 44.85; H, 3.20; N, 8.63.

GdCl$_3$(BpoA). Anal. calcd. for $C_{18}H_9Cl_3F_3GdN_4O$: C, 34.99; H, 1.47; N, 9.07. Found: C, 35.12; H, 1.55; N, 8.94.

GdCl$_3$(BpoB). Anal. calcd. for $C_{18}H_{12}Cl_3GdN_4O$: C, 38.34; H, 2.14; N, 9.94. Found: C, 38.39; H, 2.19; N, 9.89.

GdCl$_3$(BpoC). Anal. calcd. for $C_{22}H_{20}Cl_3GdN_4O$: C, 42.62; H, 3.25; N, 9.04. Found: C, 42.70; H, 3.29; N, 8.98.

OLED fabrication and measurement

EL devices were fabricated by sequentially depositing organic layers using thermal evaporation in one run under high vacuum ($<8 \times 10^{-5}$ Pa) onto a cleaned indium tin oxide (ITO) glass substrate with a sheet resistance of 7 Ω sq^{-1}. The active device area was 3 × 3 mm. The cathode was made of a 200 nm thick layer of $Mg_{0.9}Ag_{0.1}$ alloy with an 80 nm thick Ag cap. The thickness of the deposited layer and the evaporation speed of the individual materials were monitored with quartz crystal monitors. Deposition rates were maintained at 0.05–0.2 nm s^{-1} for organic materials and 0.2–0.3 nm s^{-1} for the $Mg_{0.9}Ag_{0.1}$ alloy. All electrical testing and optical measurements were performed under ambient conditions. The EL spectra were measured with a Spectra Scan PR650. The current–voltage (*I–V*) and luminance–voltage (*L–V*) characteristics were measured with a computer controlled Keithley 2400 Sourcemeter unit with a calibrated silicon diode.

Conclusions

In summary, we report the design, synthesis, and EL application of several europium complexes with phenanthroline derivatives or bipyridine derivatives as neutral ligands. Our results suggest that using tridentate neutral ligand is a viable strategy for improving the stability of lanthanide complex for deposition. By incorporating an oxadiazole moiety into the ligand with further modifying, we achieved novel complexes with characteristic emissions and high quantum yields, improved carrier transporting abilities and thermal stabilities for vapor deposition. These in turn lead to pure EL emissions and high efficiencies in appropriately configured devices. The modification of proper tridentate ligands with functional groups provides a useful guide for future work on lanthanide based OLEDs.

Acknowledgements

The authors thank the National Basic Research Program (2006CB601103) and the NNSFC (50772003, 20671006, 20821091, 90922004, 20971006) for financial support.

References

1 J. Kido and Y. Okamoto, *Chem. Rev.*, 2002, **102**, 2357.
2 J. F. Wang, R. Y. Wang, J. Yang, Z. P. Zheng, M. D. Carducci, T. Cayou, N. Peyghambarian and G. E. Jabbour, *J. Am. Chem. Soc.*, 2001, **123**, 6179.
3 Z. Q. Chen, F. Ding, F. Hao, Z. Q. Bian, B. Ding, Y. Z. Zhu, F. F. Chen and C. H. Huang, *Org. Electron.*, 2009, **10**, 939.
4 H. Xin, F. Y. Li, M. Shi, Z. Q. A. Bian and C. H. Huang, *J. Am. Chem. Soc.*, 2003, **125**, 7166.
5 H. Xin, M. Shi, X. C. Gao, Y. Y. Huang, Z. L. Gong, D. B. Nie, H. Cao, Z. Q. Bian, F. Y. Li and C. H. Huang, *J. Phys. Chem. B*, 2004, **108**, 10796.
6 U. Giovanella, M. Pasini, C. Freund, C. Botta, W. Porzio and S. Destri, *J. Phys. Chem. C*, 2009, **113**, 2290.
7 C. R. De Silva, F. Y. Li, C. H. Huang and Z. P. Zheng, *Thin Solid Films*, 2008, **517**, 957.
8 H. Xu, K. Yin and W. Huang, *Chem.–Eur. J.*, 2007, **13**, 10281.
9 J. B. Yu, L. Zhou, H. J. Zhang, Y. X. Zheng, H. R. Li, R. P. Deng, Z. P. Peng and Z. F. Li, *Inorg. Chem.*, 2005, **44**, 1611.
10 J. Kalinowski, *Opt. Mater.*, 2008, **30**, 792.

11 C. Adachi, M. A. Baldo and S. R. Forrest, *J. Appl. Phys.*, 2000, **87**, 8049.
12 Z. Q. Bian, D. Q. Gao, K. Z. Wang, L. P. Jin and C. H. Huang, *Thin Solid Films*, 2004, **460**, 237.
13 M. R. Robinson, J. C. Ostrowski, G. C. Bazan and M. D. McGehee, *Adv. Mater.*, 2003, **15**, 1547.
14 P. P. Sun, J. P. Duan, J. J. Lih and C. H. Cheng, *Adv. Funct. Mater.*, 2003, **13**, 683.
15 J. F. Fang and D. G. Ma, *Appl. Phys. Lett.*, 2003, **83**, 4041.
16 M. Sun, H. Xin, K. Z. Wang, Y. A. Zhang, L. P. Jin and C. H. Huang, *Chem. Commun.*, 2003, 702.
17 F. S. Liang, Q. G. Zhou, Y. X. Cheng, L. X. Wang, D. G. Ma, X. B. Jing and F. S. Wang, *Chem. Mater.*, 2003, **15**, 1935.
18 H. Xin, F. Y. Li, M. Guan, C. H. Huang, M. Sun, K. Z. Wang, Y. A. Zhang and L. P. Jin, *J. Appl. Phys.*, 2003, **94**, 4729.
19 M. Guan, Z. Q. Bian, F. Y. Li, H. Xin and C. H. Huang, *New J. Chem.*, 2003, **27**, 1731.
20 Z. Liu, F. S. Wen and W. L. Li, *Thin Solid Films*, 2005, **478**, 265.
21 M. D. McGehee, T. Bergstedt, C. Zhang, A. P. Saab, M. B. O'Regan, G. C. Bazan, V. I. Srdanov and A. J. Heeger, *Adv. Mater.*, 1999, **11**, 1349.
22 Z. R. Hong, C. S. Lee, S. T. Lee, W. L. Li and S. Y. Liu, *Appl. Phys. Lett.*, 2003, **82**, 2218.
23 Y. X. Zheng, J. Lin, Y. J. Liang, Y. N. Yu, Y. H. Zhou, C. Guo, S. B. Wang and H. J. Zhang, *J. Alloys Compd.*, 2002, **336**, 114.
24 Z. J. Wang and I. D. W. Sarnuel, *J. Lumin.*, 2005, **111**, 199.
25 J. B. Peng, N. Takada and N. Minami, *Thin Solid Films*, 2002, **405**, 224.
26 M. Uekawa, Y. Miyamoto, H. Ikeda, K. Kaifu and T. Nakaya, *Bull. Chem. Soc. Jpn.*, 1998, **71**, 2253.
27 M. Noto, K. Irie and M. Era, *Chem. Lett.*, 2001, 320.
28 T. Sano, M. Fujita, T. Fujii, Y. Hamada, K. Shibata and K. Kuroki, *Jpn. J. Appl. Phys.*, 1995, **34**, 1883.
29 Y. Hamada, *IEEE Trans. Electron Devices*, 1997, **44**, 1208.
30 N. Rehmann, C. Ulbricht, A. Kohnen, P. Zacharias, M. C. Gather, D. Hertel, E. Holder, K. Meerholz and U. S. Schubert, *Adv. Mater.*, 2008, **20**, 129.
31 X. H. Yang, D. C. Muller, D. Neher and K. Meerholz, *Adv. Mater.*, 2006, **18**, 948.
32 Y. T. Tao, Q. Wang, C. L. Yang, Q. Wang, Z. Q. Zhang, T. T. Zou, J. G. Qin and D. G. Ma, *Angew. Chem., Int. Ed.*, 2008, **47**, 8104.
33 E. J. Corey, A. L. Borror and T. Foglia, *J. Org. Chem.*, 1965, **30**, 288.
34 J. J. Moore, J. J. Nash, P. E. Fanwick and D. R. McMillin, *Inorg. Chem.*, 2002, **41**, 6387.
35 C. R. De Silva, J. F. Wang, M. D. Carducci, S. A. Rajapakshe and Z. P. Zheng, *Inorg. Chim. Acta*, 2004, **357**, 630.
36 C. R. De Silva, R. Y. Wang and Z. P. Zheng, *Polyhedron*, 2006, **25**, 3449.
37 C. R. De Silva, J. R. Maeyer, A. Dawson and Z. P. Zheng, *Polyhedron*, 2007, **26**, 1229.
38 C. Y. Hung, T. L. Wang, Z. Q. Shi and R. P. Thummel, *Tetrahedron*, 1994, **50**, 10685.
39 W. F. Sager, N. Filipesc and F. A. Serafin, *J. Phys. Chem.*, 1965, **69**, 1092.
40 S. I. Klink, L. Grave, D. N. Reinhoudt, F. C. J. M. van Veggel, M. H. V. Werts, F. A. J. Geurts and J. W. Hofstraat, *J. Phys. Chem. A*, 2000, **104**, 5457.
41 S. I. Klink, G. A. Hebbink, L. Grave, P. G. B. O. Alink, F. C. J. M. van Veggel and M. H. V. Werts, *J. Phys. Chem. A*, 2002, **106**, 3681.
42 G. A. Crosby, R. M. Alire and R. E. Whan, *J. Chem. Phys.*, 1961, **34**, 743.
43 G. A. Crosby and R. E. Whan, *J. Chem. Phys.*, 1962, **36**, 863.
44 X. J. Yu and Q. D. Su, *J. Photochem. Photobiol., A*, 2003, **155**, 73.
45 K. Nakamaru, *Bull. Chem. Soc. Jpn.*, 1982, **55**, 2697.
46 R. A. Campos, I. P. Kovalev, Y. Guo, N. Wakili and T. Skotheim, *J. Appl. Phys.*, 1996, **80**, 7144.
47 J. Kalinowski, W. Stampor, M. Cocchi, D. Virgili and V. Fattori, *Appl. Phys. Lett.*, 2005, **86**, 241106.
48 T. A. Hopkins, K. Meerholz, S. Shaheen, M. L. Anderson, A. Schmidt, B. Kippelen, A. B. Padias, H. K. Hall, N. Peyghambarian and N. R. Armstrong, *Chem. Mater.*, 1996, **8**, 344.
49 X. Hao, S. Mei, M. Z. Xiao, Y. L. Fu, Q. B. Zu, K. Ibrahim, Q. L. Feng and H. H. Chun, *Chem. Mater.*, 2003, **15**, 3728.
50 M. Guan, Z. Q. Bian, Y. F. Zhou, F. Y. Li, Z. J. Li and C. H. Huang, *Chem. Commun.*, 2003, 2708.
51 J. F. Weiher, L. R. Melby and R. E. Benson, *J. Am. Chem. Soc.*, 1964, **86**, 4329.

